Journal of Photochemistry and Photobiology A: Chemistry 210 (2010) 130–139

Contents lists available at ScienceDirect

Journal of Photochemistry and Photobiology A: Chemistry

journal homepage: www.elsevier.com/locate/jphotochem

Oligofluorene blue emitters for cholesteric liquid crystal lasers

L.S. Chinelatto Jr[a], J. del Barrio[a], M. Piñol[a], L. Oriol[a,*], M.A. Matranga[b], M.P. De Santo[b,**], R. Barberi[b]

[a] Departament de Química Orgánica, Facultad de Ciencias-ICMA, Universidad de Zaragoza-CSIC, Pedro Cerbuna 12, 50009-Zaragoza, Spain
[b] CEMIF.CAL, INFM CNR-Licryl Lab., Physics Department, University of Calabria, 87036 Rende (Cs), Italy

ARTICLE INFO

Article history:
Received 19 October 2009
Received in revised form
30 December 2009
Accepted 8 January 2010
Available online 18 January 2010

Keywords:
Oligofluorenes
Luminescent materials
Cholesteric liquid crystals
Photonic band gap materials
Lasers

ABSTRACT

We present the synthesis and characterization of an oligofluorene series whose chemical structure has been tuned to have amorphous nature, compatibility with liquid crystalline matrices and intrinsic chirality. Oligofluorenes are good blue emitters and the emission quantum yield is around 0.8 in the violet-blue range. The prepared materials are suitable for mirror-less laser applications based on a dye-doped liquid crystal resonator. We propose to use fluorene-based compounds to combine two necessary properties to achieve laser emission from cholesteric liquid crystal mixtures: chirality and luminescence. A good intensity emission and a fine tuning of the laser emission are demonstrated.

1. Introduction

π-Conjugated organic materials have been intensively pursued for electronics, photonics and opto-electronics. From all conjugated systems, oligofluorenes and polyfluorenes have been identified as ideal candidates for many of these applications because of their efficient blue emission, both under photo- and electric stimulation, their thermal and chemical stability but also for their potential liquid crystalline properties. In fact, many systematic structure–activity reports can be found in the literature that show the versatility of fluorene compounds in the sense that the chemical structure of the aromatic core can be easily tailored to tune a variety of properties such as colour of the emission, electronic properties or liquid crystallinity [1–4].

For sometime, we have been interested in investigating fundamental opto-electronic and photonic properties of oligofluorenes and polyfluorenes. Therefore, in addition to the primary structure–activity studies, results on liquid crystalline networks with linearly polarized blue emission from fluorene-based mono- and dimethacrylates have been reported. The films were prepared by *in situ* photopolymerization of non-emissive reactive liquid crystalline matrixes containing reactive fluorene emitters [5–7]. Also, we have verified that fluorene-based materials are ideal, due to their high quantum yield and their liquid crystals compatibility, to be used as photoluminescent dyes in mirrorless lasers technology to obtain bright laser emission in the blue-violet range [8].

Cholesteric liquid crystals (CLCs) may be considered as unidimensional photonic crystals. Since liquid crystals are highly birefringent media, the helicoidal structure present at CLCs causes a periodical modulation of the refractive indices and the presence of a selective reflection band for light propagating along the helix axis, $\Delta\lambda = p\Delta n$, where p is the helical pitch and Δn the birefringence of the medium. A comprehensive analysis of a CLC as a photonic crystal is given in the review by Kopp et al. [9].

Doping cholesterics with photoluminescent dyes is considered as a very promising way for creating compact distributed feedback lasers. In dye doped cholesteric liquid crystal (DD CLC) lasers, the cholesteric liquid crystal acts as a resonator in laser emission from doped luminescent molecules [10,11]. It is important for the development of compact lasers that the major functional elements of a mirror-less laser are combined in one cell: active medium, cavity, and tunable selector.

The existence of the selective reflection band and the ability to change smoothly the selective reflection wavelength over a wide range under the action of applied external forces make it possible to design broad band tunable lasers based on DD CLCs. In particular, tunability of lasing can be achieved in several ways: varying the temperature [11], applying a mechanical stress [12] or an electric field [13], using photo-transformation effects [14,15] and by

* Corresponding author. Tel.: +34 976762276; fax: +34 976762686.
** Corresponding author.
E-mail addresses: loriol@unizar.es (L. Oriol), desanto@fis.unical.it (M.P. De Santo).

1010-6030/$ – see front matter © 2010 Elsevier B.V. All rights reserved.
doi:10.1016/j.jphotochem.2010.01.006

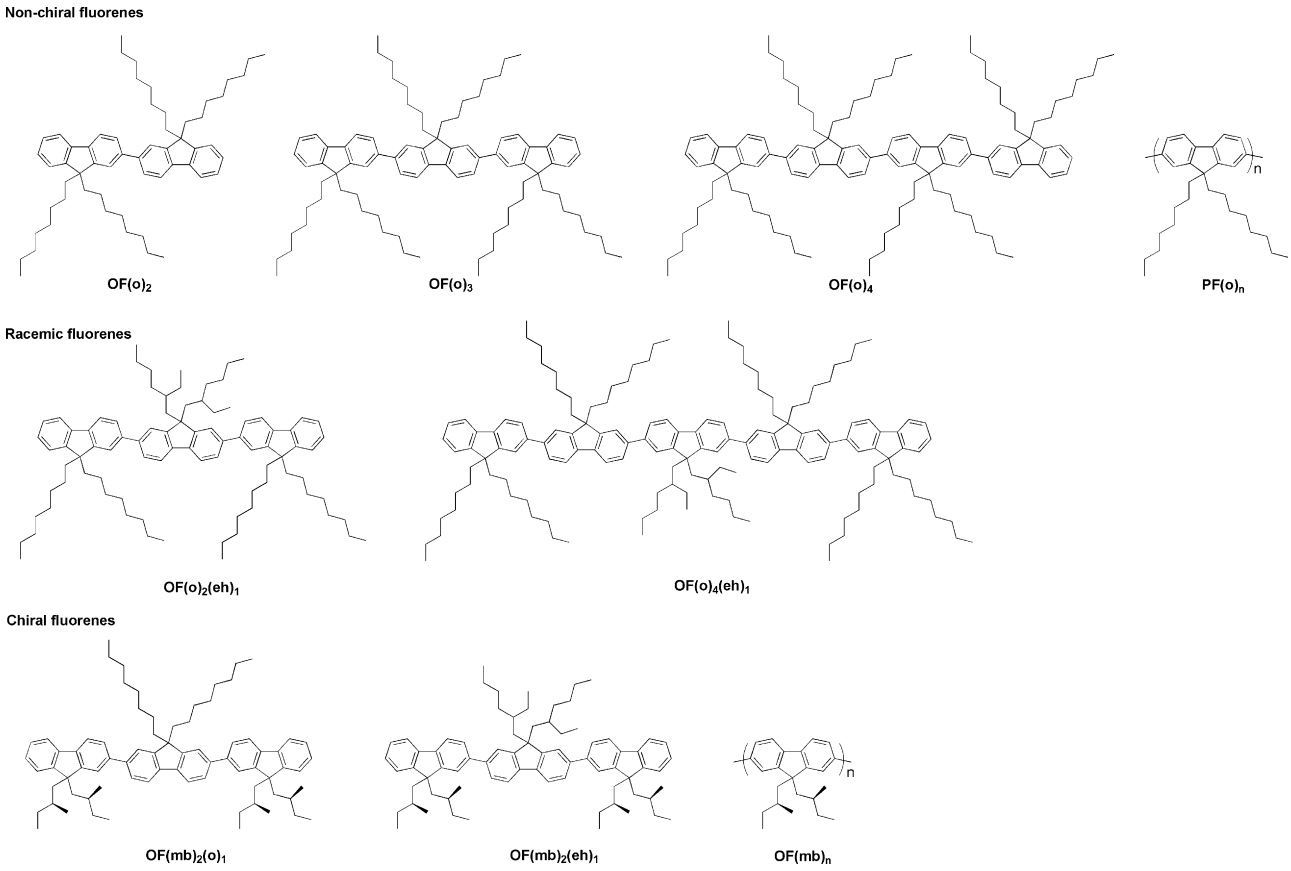

Fig. 1. Structure of the investigated oligofluorenes and polyfluorenes.

assembling cells with pitch gradient and with spatial distribution of different dyes [16,17].

It is possible to readily obtain tunable laser in the near ultraviolet through the visible spectrum to the near infrared. The broad wavelength tuning range of LC lasers, coupled with their microscopic size, narrow linewidths (<0.1 nm), and high optical efficiencies as compared with more conventional solid-state lasers, open up new applications in areas such as labs-on-a-chip, medical diagnostics, dermatology and cosmetics.

In this work we have undertaken the synthesis of a series of monodispersed oligofluorenes, both homo-oligofluorenes and co-oligofluorenes, from a dimer to a pentamer (see Fig. 1) and investigated their possible application on mirrorless lasing. In addition, we have prepared an oligomer, **OF(mb)$_n$**, of polydispersed nature and a polymer, **PF(o)$_n$** whose synthesis and properties have already been described by other authors [18]. Each fluorene unit has been functionalized at the C9 position with two pendant alkyl chains, which is critical for attaining adequate solubility and thermal behaviour. In these structures, the pendant aliphatic chains have been varied from linear to branched ones, either racemic or chiral. In terms of promoting mesomorphism, it has been proven that it is necessary to combine at least 4 fluorene units with appropriate aliphatic chains at the C9 bridging position of fluorenyl units [19]. The benefit from branching aliphatic pendant chains in comparison to linear ones has also been proved in terms of mesophase formation and crystallinity suppression. In addition, the incorporation of chirality in these aliphatic chains has been reported to give rise to helical assemblies and to cause chiroptical activity in films [20,21]. Regardless of pendant aliphatic chains, co-oligomers are more favourable to the formation of morphologically stable glassy nematics than homo-oligomers [19].

At present, DD CLCs contain at least three compounds: a nematic material, an optical active dopant and a luminescent dye, that have to be carefully selected according to their optical, solubility and thermal stability properties. Therefore, we envisaged the possibility to use fluorene-based materials that can act at the same time as chirality promoters and luminescent compounds [8]. For this purpose, we have focussed our attention mainly on those oligomers containing laterally appended chiral chains. We prove that the investigated compounds have high emission quantum yields and adequate stability. In addition, fluorenes are optically dichroic molecules in which the emission transition moments aligns within the long molecular axis [5]. Takezoe and co-workers [22,23] have shown that doping a chiral liquid crystal with a polymeric dye helps in suppressing fluctuations in the LC matrix, enhancing the order parameter. Moreover, this promotes high alignment of the transition dipoles with the local liquid crystal director, lowering the lasing threshold. In our case, the fluorene-based emitters are of oligomeric nature with scarcely tendency towards crystallization. The thermal behaviour and twisting power ability can be adjusted by structural chemical changes such as the aromatic core length and the structure of the appended lateral chain. Therefore, we show how they can be used to obtain a tuning of the laser emission.

2. Experimental

2.1. Chemicals

Chemicals and reagents were used as received from their commercial sources. Toluene, and *N,N*-dimethylformide (DMF) were dried using standard procedures. Tetrakis(triphenylphosphine) palladium(0) [$Pd(PPh_3)_4$], bis(1,4-cyclooctadiene)nickel(0) [Ni-

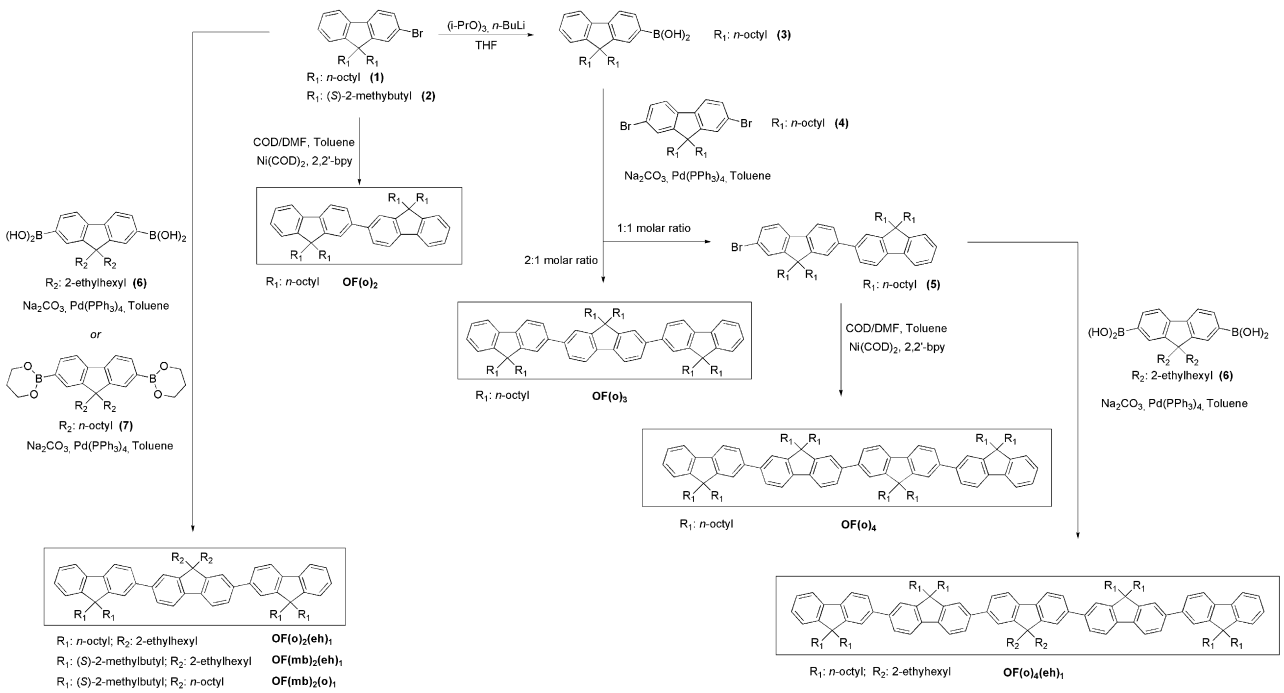

Fig. 2. Synthesis of oligofluorenes.

$(COD)_2$], 2,2-bipyridine, 1,5-ciclooctadiene (COD) were purchased from Aldrich.

The starting materials 9,9-dialkyl-1-bromofluorenes (**1**) and (**2**), 2,7-dibromo-9,9-di(*n*-octyl)fluorene (**4**) and 9,9-di(*n*-octyl) fluoren-2-yl boronic acid (**3**) were obtained following reported procedures [7,6,21]. The synthesis and characterization of 7-bromo-9,9,9′,9′-tetra(*n*-octyl)-2,2′-bifluorene (**5**) has already been reported in the literature [24]. 9,9-Bis(2-ethylhexyl) fluoren-2,7-yl diboronic acid (**6**) and 9,9-dioctylfluoren-2,7-yl-bis(trimetilen)borate (**7**) were purchased from Aldrich.

2.2. Experimental procedures and characterization data of materials

2.2.1. General synthetic procedures and characterization data for oligofluorenes

Synthetic procedures for oligofluorenes are collected in Fig. 2. **OF(o)$_2$** and **OF(o)$_4$** were obtained by the Yamamoto coupling reaction from its bromo-precursors (**1**) and (**5**), respectively, as reported for related compounds [21]. The rest of oligofluorenes, trimers **OF(o)$_3$**, **OF(o)$_2$(eh)$_1$**, **OF(mb)$_2$(o)$_1$** and **OF(mb)$_2$(eh)$_1$**, and pentamer **OF(o)$_4$(eh)$_1$** were obtained by Suzuki coupling reaction following reported procedures [19].

2.2.1.1. Characterization data ***OF(o)$_2$***. The product was prepared by Yamamoto coupling of 2-bromo-9,9-dioctylfluorene (**1**) and purified by flash column chromatography on silica gel using hexane as eluant. Finally, the target compound was isolated as a white solid in a 72% yield. IR (KBr, cm^{-1}) ν: 1609, 1466 (Ar, C–C), 884, 822, 738 (Ar). ^{1}H RMN (400 MHz, $CDCl_3$): δ (ppm) 7.79–7.73 (m, 4H), 7.65–7.62 (m, 4H), 7.38–7.33 (m, 6H), 2.09–2.01 (m, 8H), 1.27–1.09 (m, 40H), 0.82 (t, J = 7.3 Hz, 12H), 0.74–0.66 (m, 8H). ^{13}C RMN (100 MHz, $CDCl_3$): δ (ppm) 151.44, 150.99, 140.83, 140.53, 140.30, 126.95, 126.77, 126.03, 122.94, 121.41, 119.83, 119.67, 55.18, 40.35, 31.77, 30.02, 29.19, 23.82, 22.57, 14.02. Elem. Anal. Calcd for $C_{58}H_{82}$: C, 89.39; H, 10.61: Found: C, 89.36; H, 10.62. EM (FAB^+) m/z (%): 778.7 (100 $[M]^+$); MM calcd: 778.64.

2.2.1.2. Characterization data for ***OF(o)$_3$***. The product was prepared from 2,7-dibromo-9,9-dictylfluorene (**4**) and 9,9-bis(n-octyl)fluoren-2-yl boronic acid (**3**). The crude was purified using MPLC on silica gel using hexane/ethyl acetate 10:1 as eluant to give the product as a white solid in a 55% yield. IR (KBr, cm^{-1}) ν: 1608, 1580 (Ar, C–C); 883, 778, 739 (Ar). ^{1}H RMN (400 MHz, $CDCl_3$): δ (ppm) 7.85–7.74 (m, 6H), 7.64–7.71 (m, 8H), 7.30–7.41 (m, 6H), 2.18–2.10 (m, 10H), 1.32–1.18 (m, 62H), 0.90 (t, J = 7.3 Hz, 18H), 0.88–0.87 (m, 12H). ^{13}C RMN (100 MHz, $CDCl_3$): δ (ppm) 151.80, 151.49, 151.04, 140.84, 140.56, 140.54, 140.35, 140.01, 126.97, 126.79, 126.15, 126.05, 122.94, 121.51, 121.44, 119.91, 119.85, 119.70, 55.19, 40.37, 31.78, 30.04, 29.19, 23.92, 23.84, 22.57, 14.02. Elem. Anal. Calcd for $C_{87}H_{122}$: C, 89.47; H, 10.53. Found: C, 89.44; H, 10.51. EM (FAB^+) m/z (%):1166.90 (100 $[M]^+$); MM calcd: 1166.95.

2.2.1.3. Characterization data for ***OF(o)$_4$***. The product, obtained by Yamamoto coupling of 7-bromo-9,9,9′,9′-tetrakis(*n*-octyl)-2,2′-bifluorene (**5**), was isolated as a white solid after purifying the reaction crude by flash column chromatography on silica gel using hexane/dichloromethane 9:1 as eluant in a 82% yield. IR (nujol, cm^{-1}) ν: 1608, 1581 (Ar, C–C); 884, 779, 739 (Ar). ^{1}H RMN (400 MHz, $CDCl_3$): δ (ppm) 7.88–7.66 (m, 20H), 7.43–7.30 (m, 6H), 2.18–1.98 (m, 16H), 1.29–1.09 (m, 80H), 0.82 (t, J = 7.1 Hz, 24H), 0.76–0.66 (m, 16H). ^{13}C RMN (100 MHz, $CDCl_3$): δ (ppm) 151.78, 151.46, 150.99, 140.78, 140.51, 140.46, 140.32, 140.00, 139.97, 126.97, 126.76, 126.13, 126.02, 125.99, 122.90, 121.46, 121.38, 119.92, 119.86, 119.70, 55.31, 55.15, 40.37, 31.78, 30.03, 30.02, 29.21, 23.89, 23.81, 22.58, 14.05. Elem. Anal. Calcd for $C_{116}H_{162}$: C, 89.51; H, 10.49. Found: C, 89.41; H, 10.81. EM (MALDI-TOF, dithranol) m/z (%): 1555.4 (100 $[M]^+$); MM calcd: 1555.27.

2.2.1.4. Characterization data for ***OF(o)$_2$(eh)$_1$***. The product was obtained by Suzuki coupling of 2-bromo-9,9-bis(*n*-octyl)fluorene (**1**) and 9,9-bis(2-ethylhexyl)fluoren-2,7-diyl-boronic acid (**6**). It was purified by MPLC using hexane as eluant and gradually increasing polarity with dichloromethane. The target compound was isolated as a viscous colourless liquid in 54% yield. IR (KBr, cm^{-1}) ν: 3022 (Ar, C–H); 2983 (C–H); 1610 (Ar, C–C); 823 (Ar). ^{1}H

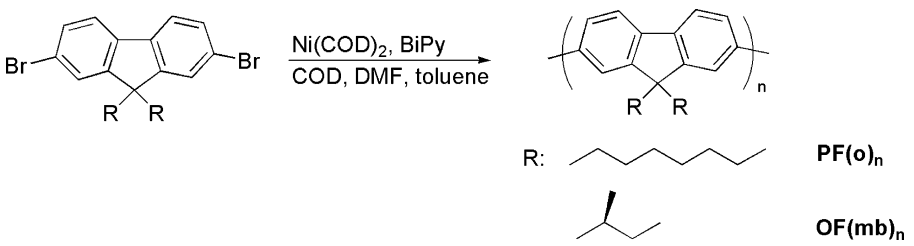

Fig. 3. Synthesis of **PF(o)$_n$** and **OF(mb)$_n$**.

RMN (400 MHz, $CDCl_3$): δ (ppm) 7.92–7.74 (m, 6H), 7.74–7.58 (m, 8H), 7.47–7.28 (m, 6H), 2.28–1.91 (m, 12H), 1.38–1.06 (m, 35H), 1.06–0.51 (m, 55H). ^{13}C RMN (100 MHz, $CDCl_3$): δ (ppm) 151.3, 151.2, 151.0, 140.8, 140.8, 140.7, 140.2, 140.0, 128.7, 127.1, 126.9, 126.2, 125.9, 125.8, 122.9, 121.4, 119.8, 119.7, 55.1, 55.0, 40.4, 40.3, 34.7, 33.9, 31.8, 30.1, 29.2, 28.2, 28.2, 27.3, 23.8, 22.7, 22.6, 14.0, 10.5, 10.4. Elem. Anal. Calcd for $C_{87}H_{122}$: C, 89.50; H, 10.50. Found: C, 89.20; H, 10.80. EM (MALDI-TOF, dithranol) m/z (%): 1166.9 (100 $[M]^+$); MM calcd: 1166.95.

2.2.1.5. Characterization data for ***OF(o)$_4$(eh)$_1$***. The product was obtained by Suzuki coupling of 7-bromo-9,9,9′,9′-tetrakis(*n*-octyl)-2,2′-bifluorene (**5**) and 9,9-bis(2-ethylhexyl)fluoren-2,7-diyl-boronic acid (**6**). It was purified by MPLC using hexane as eluant and gradually increasing polarity with dichloromethane. The target compound was isolated as a white solid in 71% yield. IR (KBr, cm^{-1}) ν: 1608, 1456 (Ar, C–C); 815 (Ar). ^{1}H RMN (400 MHz, $CDCl_3$): δ (ppm) 7.90–7.40 (m, 10H), 7.40–7.57 (m, 16H), 7.43–7.30 (m, 6H), 2.25–1.93 (m, 20H), 1.34–1.03 (m, 84H), 1.03–0.52 (m, 66H). ^{13}C RMN (100 MHz, $CDCl_3$): δ (ppm) 151.8, 151.7, 151.5. 151.4, 151.3, 140.9, 140.7, 140.2, 140.0, 139.8, 128.8, 127.2, 127.1, 126.9, 126.3, 126.0, 125.9, 123.0, 121.5, 121.4, 121.3, 119.9, 119.6, 119.6, 55.3, 55.2, 55.1, 40.4, 40.3, 34.8, 34.0, 34.0, 31.8, 30.0, 29.2, 28.2, 28.2, 27.3, 27.1, 23.9, 23.8, 22.8, 22.8, 22.6, 14.1, 10.5, 10,5, 10.4. Elem. Anal. Calcd for $C_{145}H_{202}$: C, 89.53; H, 10.47. Found: C, 89.35; H, 10.70. EM (MALDI-TOF, dithranol) m/z (%): 1944.3 (100 $[M+1]^+$); MM calcd: 1943.58.

2.2.1.6. Characterization data for ***OF(mb)$_2$(o)$_1$***. The product was obtained by Suzuki coupling of 2-bromo-9,9-bis[(*S*)-2-methylbutil]fluorene (**2**) and 9,9-bis(*n*-octyl)fluoren-2,7-diyl-bis(trimetilen)borate (**7**). It was purified by MPLC using hexane as eluant and gradually increasing polarity with dichloromethane. The target compound was isolated as a viscous colourless liquid in 67% yield. IR (KBr, cm^{-1}) ν: 1611, 1507 (Ar, C–C); 814 (Ar). ^{1}H RMN (400 MHz, $CDCl_3$): δ (ppm) 7.93–7.67 (m, 14H), 7.57–7.35 (m, 6H), 2.36–1.96 (m, 12H), 1.34–1.15 (m, 28H), 1.04–0.67 (m, 26H), 0.43–0.38 (m, 12H). ^{13}C RMN (100 MHz, $CDCl_3$): δ (ppm) 151.8, 151.3, 150.9, 141.7, 140.9, 140.6, 140.4, 140.1, 128.8, 127.2, 126.6, 126.8, 126.1, 123.9, 122.5, 121.6, 119.9, 119.7, 54.8, 48.0, 47.7, 40.2, 31.8, 31.2, 31.2, 30.0, 30.6, 29.2, 29.2, 22.6, 21.2, 14.1, 11.0. Elem. Anal. Calcd for $C_{75}H_{98}$: C, 90.12; H, 9.88. Found: C, 89.38; H, 10.11. EM (MALDI-TOF, dithranol) m/z (%): 770.7 (100), 998.8 (80 $[M]^+$); MM calcd: 998.77.

2.2.1.7. Characterization data for ***OF(mb)$_2$(eh)$_1$***. The product was obtained by Suzuki coupling of 2-bromo-9,9-bis[(*S*)-2-methylbutil]fluorene (**2**) and 9,9-bis(2-ethylhexyl)fluoren-2,7-diyl-boronic acid (**6**). It was purified by MPLC using hexane as eluant and gradually increasing polarity with dichloromethane. The target compound was isolated as a viscous colourless liquid in 59% yield. IR (KBr, cm^{-1}) ν: 1607, 1508 (Ar, C–C); 818 (Ar). ^{1}H RMN (400 MHz, $CDCl_3$): δ (ppm) 7.88–7.70 (m, 14H), 7.55–7.34 (m, 6H), 2.38–1.96 (m, 12H), 1.10–0.84 (m, 24H), 0.83–0.61 (m, 30H), 0.40–0.37 (m, 12H). ^{13}C RMN (100 MHz, $CDCl_3$): δ (ppm) 151.2, 151.1, 150.8, 141.9 141.0, 140.3, 140.2, 139.5, 128.7 127.1, 126.8, 126.5, 126.1 126.0, 123.9, 123.0 119.9, 119.7, 55.1, 54.7, 48.0, 44.2, 34.7, 34.3, 31.3, 30.5, 28.3, 27.3, 22.7, 21.1, 14.0, 11.0, 10.4. Elem. Anal. Calcd for $C_{75}H_{98}$: C, 90.12; H, 9,88. Found: C, 89.60; H, 10.04. EM (MALDI-TOF, dithranol) m/z (%):770.6 (100), 998.7 (80 $[M]^+$); MM calcd: 998.77.

2.2.2. General polymerization procedure and characterization data for ***PF(o)$_n$*** *and* ***OF(mb)$_n$***

The procedure is gathered in Fig. 3. A Schlenk was charged with $Ni(COD)_2$ (2.146 mmol) and 2,2′-bipyridine (2.145 mmol) in a glove box and then purged with argon. DMF (8 mL) and COD (2.146 mmol) were added and the solution subsequently heated at 70 °C for 30 min. Finally, the 2,7-dibromofluorene (1.823 mmol) dissolved in toluene (8 mL) was added and the reaction vigorously stirred at 70 °C for 24 h. The polymer was isolated from the reaction crude by flash column chromatography over silica gel using hexane as eluant.

2.2.2.1. Characterization data for ***PF(o)$_n$***. The polymer was isolated as a yellow powder in 48% yield. GPC (THF, polystyrene standards): Mw 19,046, Mn 12,763, polydispersity 1.5. IR (KBr, cm^{-1}) ν: 3019 (Ar–H), 2988 (C–H), 1609, 1457 (ArC–C), 813 (Ar). ^{1}H NMR (400 MHz, $CDCl_3$) δ (ppm): 7.84 (d, J = 8.1 Hz, 2H,), 7.74–7.60 (m, 4H), 2.21–1.96 (m, 4H), 1.25–1.03 (m, 20H), 0.91–0.60 (m, 10H). ^{13}C RMN (100 MHz, $CDCl_3$): δ (ppm) 151.82, 140.52, 140.00, 126.15, 121.53, 120.04, 55.34, 40.49, 31.87, 30.08, 29.26, 23.95, 22.62, 14.10. Elem. Anal. Calcd for $C_{29}H_{40}$: C, 89.61; H, 10.39. Found: C, 89.45; H, 10.55.

2.2.2.2. Characterization data for ***OF(mb)$_n$***. The compounds were isolated as a white powder in 69% yield. GPC (THF, polystyrene standards): Mw 7725, Mn 4798, polydispersity 1.6. IR (KBr, cm^{-1}) ν: 3024 (Ar–H); 2961, 2929 (C–H), 1611, 1460 (ArC–C), 814, 740 (Ar). ^{1}H NMR (400 MHz, $CDCl_3$) δ (ppm): 7.95–7.79 (m, 2H), 7.79–7.60 (m, 4H), 2.37–2.15 (m, 2H), 2.07–1.88 (m, 2H), 1.09–0.78 (m, 6H), 0.76–0.59 (m, 6H), 0.47–0.22 (m, 6H). ^{13}C RMN (100 MHz, $CDCl_3$): δ (ppm) 151.50, 140.20, 130.12, 127.13, 122.75, 121.24, 54.99, 47.67, 31.28, 21.66, 20.98, 11.93. Elem. Anal. Calcd for $C_{23}H_{28}$: C, 90.71; H, 9.29. Found: C, 90.27; H, 9.73.

2.3. Preparation of films

Thin films of polymers **PF(o)$_n$** and **OF(mb)$_n$** were deposited on 1 cm^2 glass squares by spin-coating (at 2000 rpm speed for 60 s) from 0.5 mL of a solution of the polymer in THF (1 g/L).

Films of oligofluorenes were prepared by *in situ* photopolymerization of reactive nematic blends that contained a non-emissive liquid crystalline matrix and the oligofluorene in 95:5 molar ratio [5–7,25]. The liquid crystalline matrix contained 1,2-di[4-(6-acryloyloxyhexyloxy)benzoyloxy]-2-methylbenzene (C6M) and 1-[4-(6-acryloyloxyhexyloxy)benzoyloxy]-2-methyl-4-(4-octylbenzoyloxy)benzene (C6Mm) in 10:85 molar ratio. C6M

Table 1
Thermal characterization of oligofluorenes and polyfluorenes.

Compound	TGA[a]	Residue at 600 °C[b]	Thermal transitions[c]
OF(o)$_2$	374	0	g –20 I
OF(o)$_3$	417	10	g –1 I[d]
OF(o)$_2$(eh)$_1$	392	9	g –13 I
OF(mb)$_2$(o)$_1$	380	24	g 10 I
OF(mb)$_2$(eh)$_1$	345	17	g 11 I
OF(o)$_4$	421	37	g 11 I[e]
OF(o)$_4$(eh)$_1$	396	32	g 0 I
PF(o)$_n$	425	43	C 139 (9.74) N 224 (–)[f] I
OF(mb)$_n$	402	47	C 210 (–)[f] Ch > 250–300 (–)[f] I[dec.]

[a] Decomposition temperature given in °C at the onset of the weight loss curve.
[b] Pyrolysis residue at 600 °C determined from the weight loss curve.
[c] g: glass; C: crystal; I: isotropic liquid; N: nematic; Ch: cholesteric. Temperatures are given in °C and correspond to a second heating of the sample at 20 °C/min. Values in brackets correspond to enthalpy transitions given in kJ/mol.
[d] The as obtained sample is a semicrystalline solid with a melting temperature of 58 °C and an associated enthalpy of 41.6 kJ/mol.
[e] The as obtained sample is a semicrystalline solid with a melting temperature of 57 °C and an associated enthalpy of 32.2 kJ/mol.
[f] POM data.

shows a maximum absorbance at 268 nm and C6Mm at 265 nm, both determined in THF. The photopolymerizable mixtures were prepared by dissolving the components together with 1% (w/w) of the photoinitiator Irgacure 784-DC® and 200 ppm of the thermal inhibitor 2,6-di-*tert*-butyl-4-methylphenol in freshly distilled dichloromethane. The solvent was evaporated at room temperature and residual solvent was removed under vacuum. During their preparation, storage and handling, the samples were suitably protected and kept away from light. The blends present a Nematic phase between 60 and 125 °C. Films were produced by irradiation at 60 °C during 10 min of the molten sample inside a commercial LC cell (Linkam 5 μm) in a thermostatic stage at a controlled temperature using an OSRAM Ultravitalux 300 W lamp using both a 400 nm long-pass filter and an IR filter between the lamp and the sample. The irradiation source was located 20 cm from the cell. The cells were filled by capillary action at 80–100 °C and cooled down to the polymerization temperature.

2.4. Instrumentation

Infrared spectra were measured on an ATI-Matsson Genesis Series FTIR from either nujol mulls between NaCl disks or KBr pellets. ^{1}H NMR and ^{13}C NMR spectra were recorded on a Bruker AV-400 operating at 400 or 100 MHz. Elemental analysis was performed with a Perkin-Elmer 240C microanalyzer. Matrix-assisted laser desorption ionization-time-of-flight mass spectrometry (MALDI-TOF-TOF) was performed at the Sidi Service of the Universidad Autónoma (Madrid) on a 4700 Proteomic analyzer from Applied Biosystems using dithranol as a matrix and, when required, sodium iodide as a cationic agent matrix. Fast atom bombardment (FAB) mass spectrometry was performed on a VG Autospec from Waters using 3-nitrobenzyl alcohol as a matrix. Molecular weights were determined by gel permeation chromatography (GPC) using a Waters liquid chromatography system equipped with 600E multisolvent delivery system and a 996 photodiode array detector. Polymers were eluted with THF at 0.8 mL/min flow rate using a combination of two Ultrastyragel® columns with pore size of 500 and 10^4 Å and, they were calibrated using polystyrene standards.

The optical textures of the mesophases were studied with an Olympus BH-2 polarizing microscope equipped with a Linkam THMS600 hot stage and a CS196 cooling system. Differential scanning calorimetry (DSC) was performed using a DSC Q2000 from TA Instruments with samples sealed in aluminium pans at a scanning rate of 20 °C/min under a nitrogen atmosphere. Temperatures were read at the maximum of the transition peaks, and the glass transition temperature was read at the midpoint of the heat capacity increase. Thermogravimetric analysis (TGA) was performed at 10 °C/min under nitrogen atmosphere using a TGA Q5000IR from TA Instruments. TGA data are given as the onset of the decomposition curve.

UV–vis absorption spectra were measured with a UV4-200 from ATI-Unicam using 10^{-4}–10^{-5} M solutions in THF. Fluorescence spectra were measured with a Perkin-Elmer LS50B spectrofluorimeter using solutions in THF of ca. 0.01 absorbance (about 10^{-6}–10^{-7} M) under excitation at the absorption maximum. Emission quantum yields (ϕ_{em}) were measured relative to 9,10-diphenylanthracene (ϕ_{em} = 0.90 in cyclohexane) [26] from corrected emission spectra.

3. Results and discussion

3.1. Synthesis and thermal characterization

The oligofluorene cores have been built up by a synthetic strategy based on aryl–aryl coupling reactions of Suzuki or Yamamoto types, as it is shown in Fig. 2. The Yamamoto homocoupling of aryl bromides catalyzed by nickel(0) is a very effective synthetic alternative that it is only viable when cores with an even number of fluorenyl units are required. Therefore, dimer **OF(o)$_2$** and tetramer **OF(o)$_4$** were prepared by Yamamoto coupling reaction from the corresponding monobrominated precursors, (**1**) and (**5**) respectively, in 72–82% yields.

Suzuki Pd-catalyzed heterocoupling between aryl halides and aryl boronic acids has been described as a very versatile route that uses mild reaction conditions and tolerates water and different functional groups [27]. This alternative has been used to synthesize cores with an odd number of fluorenyl units, i.e. trimers and pentamers, by coupling a monofunctional fluorene with a difunctional fluorene in a 2:1 stochiometric ratio. Two alternatives have been employed depending on available starting materials. Either a dibromofluorene was coupled to a fluorenyl boronic acid (Br–F–Br and F–B(OH)$_2$ respectively, where F stands for a fluorenyl core) or, otherwise, a bromofluorene was coupled to a fluorenyl diboronic acid (F–Br and B(OH)$_2$–F–B(OH)$_2$). The reaction was conducted in toluene at 90 °C using a slight excess of the monofunctional reactant (approx. 10% molar), Pd(PPh$_3$)$_4$ (5% molar of the boronic acid) and 2 M Na_2CO_3 (fivefold of the molar amount of the boronic acid) for 48 h in 50–60% yields. Nevertheless, we have encountered important difficulties within the purification of the final products, which require the use of preparative chromatographic techniques, such as medium pressure liquid chromatography (MPLC).

Polyfluorenes **PF(o)$_n$** and **OF(mb)$_n$** were synthesized according to Yamamoto polymerization nickel(0) mediated process of the corresponding 9,9-dialkyl-2,7-dibromofluorene monomers in 48% and 69 yields, respectively as it is outlined in Fig. 3 [28]. **PF(o)$_n$** and

OF(mb)$_n$ have weight-average molecular weights (Mw) of about 19,046 and 7725, respectively, with polydispersities around 1.5–1.6 according to GPC analysis against polystyrene standards.

The structure of these oligomers and polymers was elucidated mainly by ^{1}H and ^{13}C NMR spectroscopies and MALDI-TOF spectrometry.

Thermal stability was evaluated by thermogravimetric analysis (TGA) and relevant data are collected in Table 1. Weight loss curves rule out the presence of low boiling point contaminants and massive weight loss associated with thermal decomposition of the samples was detected above 350 °C. It is worth mentioning that in this series thermal stability increases with the number of fluorene units as well as the pyrolysis residue. Besides, results imply that, for the same number of fluorene units, branched lateral chains slightly reduce thermal stability. Thus, the onset decomposition temperature decreases from 417 °C for **OF(o)$_3$** to 392 °C for **OF(o)$_2$(eh)$_1$**, 380 °C for **OF(mb)$_2$(o)$_1$** and 345 °C for **OF(mb)$_2$(eh)$_1$**.

Thermal and mesomorphic behaviour was investigated by DSC and POM; data are summarized in Table 1. Oligofluorenes, from dimer to pentamer, are obtained either as waxy solids or semicrystalline solids that, once melted, are difficult to crystallize. DSC traces show for all the oligomers a jump in the baseline at temperatures between −20 and 10 °C corresponding to the glass transition temperature (Tg). As it is expected, Tg increases with the length of the π-core. For instance, Tg values for **OF(o)$_2$**, **OF(o)$_3$** and **OF(o)$_4$** increase from −20 to −1 °C and 11 °C, respectively. In relation to the effect of branching, comparison of different trimers suggests that a tendency is not straightforward. When *n*-octyl chains are substituted in **OF(o)$_3$** by 2-ethylhexyl ones in **OF(o)$_2$(eh)$_1$** Tg goes down from −1 to −13 °C. However, as the Tg value of the corresponding OF(eh)$_3$ has been reported to be 1 °C [28], the decrease is probably due to disturbance of structural uniformity within the co-oligofluorene more than to structural differences between *n*-octyl and 2-ethylhexyl chains. On the contrary, incorporation of shorter 2-(*S*)-methylbutyl chains increases the Tg up to 10 and 11 °C for **OF(mb)$_2$(o)$_1$** and **OF(mb)$_2$(eh)$_1$**, respectively. Chen and co-workers, who investigated a series of 9,9-bis(2-(*S*)-methylbutyl) substituted oligofluorenes, determined for the corresponding trimer **OF(mb)$_3$** a Tg value of 40 °C [21]. This indicates that this shorter and branched chain increase Tg when compared to *n*-octyl and 2-ethylhexyl chains.

There are several reports on literature concerning with the relationship between structural factors (size of the π-core and type of alkyl chain appended at C9) and mesomorphism [3,18,28]. According to them it is necessary to combine at least 4 or 5 fluorene units with appropriate alkyl chains. In this sense, branched alkyl chains are preferred over lineal ones and from them, 2-ethylhexyl over 2-(*S*)-methylbutyl. In spite of this background, none of the oligofluorenes investigated herein are liquid crystal but, because of their amorphous nature, they are expected to be compatible with liquid crystalline matrices.

The polymers **PF(o)$_n$** and **OF(mb)$_n$** are liquid crystals. In accordance with previous reports, **PF(o)$_n$** develops a fairly fluid Nematic phase from 140 to 224 °C [18]. The DSC curves of **OF(mb)$_n$** do not show clear transitions, however when viewed under POM clearly melts into a liquid crystal phase at around 160 °C that is stable up to 250–300 °C; transition into the isotropic liquid goes along with thermal degradation of the sample. In agreement with observations for monodispersed oligofluorenes by Chen and co-workers, the mesophase can be assigned to a cholesteric one [20,21].

3.2. Optical properties in dilute solution and film

The optical properties, absorption and emission spectra, were first evaluated in THF solution and results are shown in Table 2. The general trends observed in absorption and emission properties in relation to the conjugation length are consistent with reports on these type of systems in which the number or type of the pendant chains do not have a significant influence [3,29]. Oligofluorenes and polyfluorenes show an unstructured absorption band above 330 nm due to π–π* transition. Emission spectra of oligofluorenes have narrower and more structured bands with several maxima in the violet-blue region of the visible spectrum [28]. Emission efficiencies were calculated to be 0.6–0.8 for the investigated compounds. Absorption and emission bands are red-shifted

Table 2
Absorption and emission properties of oligofluorenes and polyfluorenes in THF solution.

Compound	λ_{abs} (nm) [log ε ($M^{-1}cm^{-1}$)]	λ_{em} (nm)[a]	Φ_{em}
OF(o)$_2$	330 [4.72]	365, 383	0.63
OF(o)$_3$	353 [4.94]	395, 417	0.75
OF(o)$_2$(eh)$_1$	355 [4.87]	395, 416	0.80
OF(mb)$_2$(o)$_1$	350 [4.82]	394, 412	0.80
OF(mb)$_2$(eh)$_1$	351 [4.84]	396, 412	0.81
OF(o)$_4$	360 [5.07]	406, 430	0.77
OF(o)$_4$(eh)$_1$	365 [5.08]	411, 432^{sh}	0.82
PF(o)$_n$	379 [–]	419, 439^{sh}	0.80
OF(mb)$_n$	373 [–]	414, 435^{sh}	0.78

[a] λ_{em} registered when excitation at λ_{abs}; sh: shoulder.

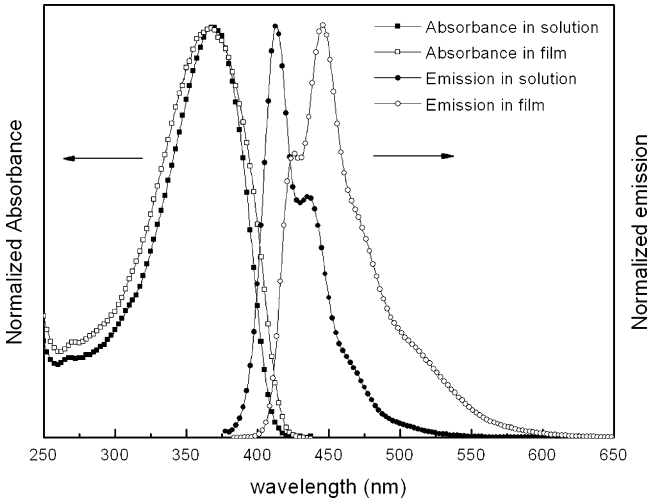

Fig. 4. Absorption and emission spectra of **OF(mb)$_n$** in solution and film.

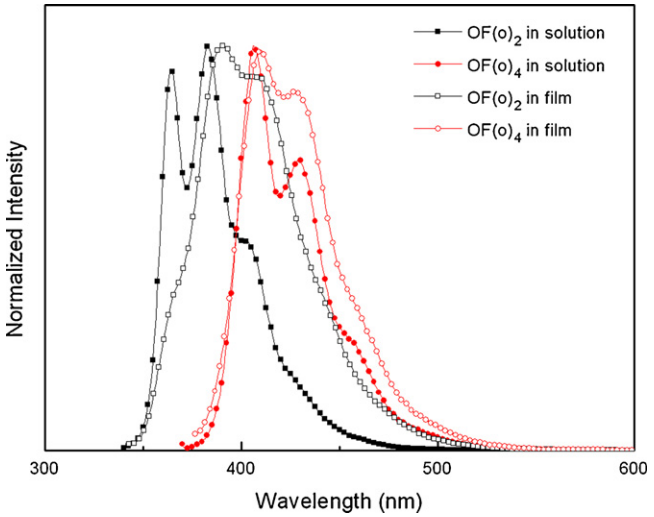

Fig. 5. Emission spectra of **OF(o)$_2$** and **OF(o)$_4$** in solution and film.

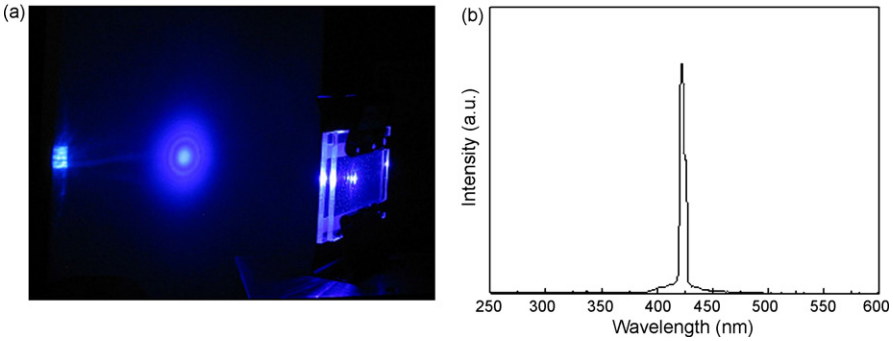

Fig. 6. (a) Laser spot from a CLC mixture doped with **OF(o)$_3$**. (b) Laser emission from the mixture containing **OF(o)$_3$**.

on increasing the length of the aromatic core up to the effective conjugation length, which has been estimated in 12–14 fluorene units for absorption and 6 fluorene units for emission [28,29]. Correlation of these data points towards the oligomeric nature of **OF(mb)$_n$**, as otherwise was presumed from GPC measurements (see Section 3.1). Extrapolation using published data for monodispersed oligomers gives an average of 6–7 fluorene units for this compound [21].

The optical properties of thin films of **PF(o)$_n$** and **OF(mb)$_n$** prepared by spin-coating were also investigated (Fig. 4). Absorption spectra of films are similar in λ_{abs} to those observed in solution although the bandwidth is slightly broadened. Some authors have related the spectral broadening with the formation of ground state aggregates by interchain π–π^* interactions, which in turn increases the effective conjugation [30]. Film emission spectra are 10–11 nm red-shifted from their solution spectra and the same time that relative intensity of the low energy transition increases, presumably due to a more planar excited state in solid state [30].

Because of their low Tg values, the synthesized oligofluorenes do not form films of optimal quality at room temperature; therefore, optical properties in solid were evaluated by dispersing them in a liquid crystalline network processed by *in situ* photopolymerization. Therefore, a non-emissive reactive Nematic matrix was used where the oligofluorene (5% molar) was dispersed [5–7,25]. The reactive blends where photopolymerized using visible light inside a glass cell at 60 °C giving transparent films of good optical quality.

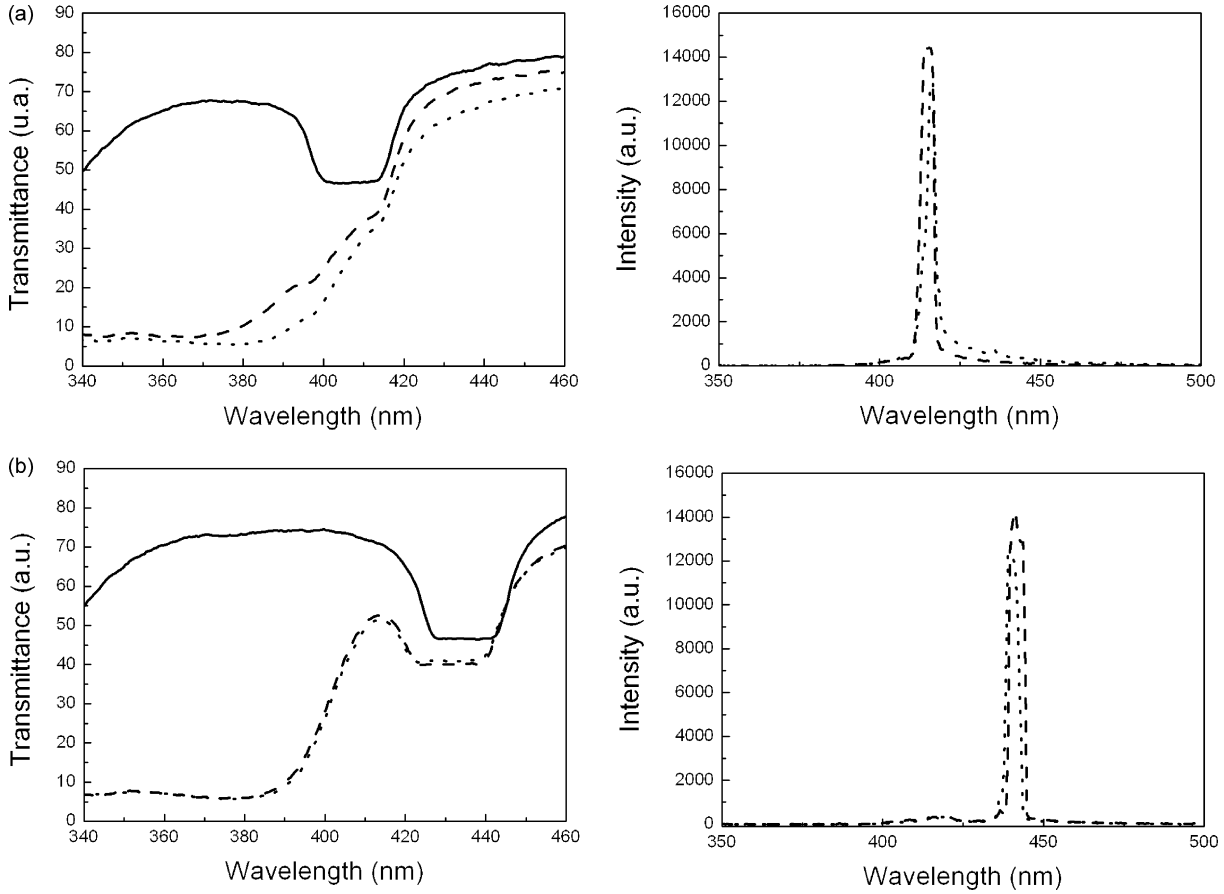

Fig. 7. Photonic band gap and laser emission for **OF(mb)$_2$(o)$_1$** doped mixtures: (a) Photonic band gap (left) for the mixture 62% **MLC-6816** + 38% **MLC-6247** (solid line) doped with 0.5% of **OF(mb)$_2$(o)$_1$** (dashed line) and with 1% of the same compound (dotted line) and the laser peaks (right) emitted from the doped mixtures. (b) Photonic band gap (left) for the mixture 64.5% **MLC-6816** + 35.5% **MLC-6248** (solid line) doped with 0.5% of **OF(mb)$_2$(o)$_1$** (dashed line) and with 1% of the same compound (dotted line) and the laser peaks (right) emitted from the doped mixtures.

Emission spectra for the films were recorded having similar features to those recorded from solution (see Fig. 5). The emission bands, broader and less structured than in solution, are slightly red-shifted more remarkable for **OF(o)$_2$**.

3.3. Lasing from CLC mixtures containing fluorene-based compounds

Investigated DD CLCs contain a nematic material, an optical active dopant and the fluorene luminescent dye. As nematic materials **MLC-6815** and **MLC-6816** were used. **MLC-6247** and **MLC-6248** were used, respectively, as left hand and right hand chiral dopants. These mixtures were purchased from Merck. CLC cells were prepared using two glass plates covered with a layer of antiparallel rubbed PVA (polyvinylalcohol).

Investigations on photoexcitation were performed using as a source a nitrogen laser, Model VSL-337ND-S (Spectra Physics). The pulse wavelength, width, and repetition rate were 337 nm, 4 ns, and 1–10 Hz, respectively. The laser beam was focused by a lens $f = 10$ cm to reduce the spot size onto the cell to few hundreds of micrometers. The pump beam hits the sample at 45° with respect to the cell normal, a usual experimental geometry for this kind of experiment. An optical fibre coupled to the spectrometer Avantes Fiberoptics Model AVASPEC-2048, with 1.4 nm resolution, collected the light emitted from the sample.

Fluorene-based materials are ideal to be used as photoluminescent dyes to obtain bright laser emission in the blue-violet range. As an example, a cell where the non-chiral **OF(o)$_3$** was used as photoluminescent dye was measured. The cell was filled with the mixture 99.4% [62% **MLC-6816** + 38% **MLC-6247**] + 0.6% **OF(o)$_3$**. In Fig. 6a, it is clearly visible a bright blue emission from the CLC cell. The spectrum of the laser emission is shown in Fig. 6b. The laser efficiency is quite high, around 10%, and the laser linewidth is estimated about 5–6 nm.

Small amounts of the chiral luminescent dyes **OF(mb)$_2$(o)$_1$**, **OF(mb)$_2$(eh)$_1$** and **OF(mb)$_n$**, were added to conventional chiral mixtures. These amounts of the luminescent dye allow to twist or to untwist the cholesteric helix, shifting accordingly the photonic stop band position, and then to obtain a fine tuning of the laser emission. Indeed, the tuning can only be achieved in a narrow range of wavelengths inside the fluorescence band of the fluorene-based materials.

The starting cholesteric mixtures were prepared to have a suitable helical pitch so that the photonic band gap could match the luminescence band of the chromophore. Several right and left hand cholesteric mixtures were prepared to be doped with the chiral fluorene-based compounds, **OF(mb)$_2$(o)$_1$**, **OF(mb)$_2$(eh)$_1$** and **OF(mb)$_n$**, in order to verify their handedness and to evaluate the effect in the photonic stop band shift as well as on the laser emission.

In Fig. 7 it is shown that the effect of the doping of a left hand (top) and right hand (bottom) mixtures of cholesterics with a small amount of **OF(mb)$_2$(o)$_1$**. In particular in Fig. 7a it is shown the photonic band gap shift obtained doping the mixture 62% **MLC-6816** + 38% **MLC-6247** (solid line) with 0.5% of **OF(mb)$_2$(o)$_1$** (dashed line) and with 1% of the same compound (dotted line) and the

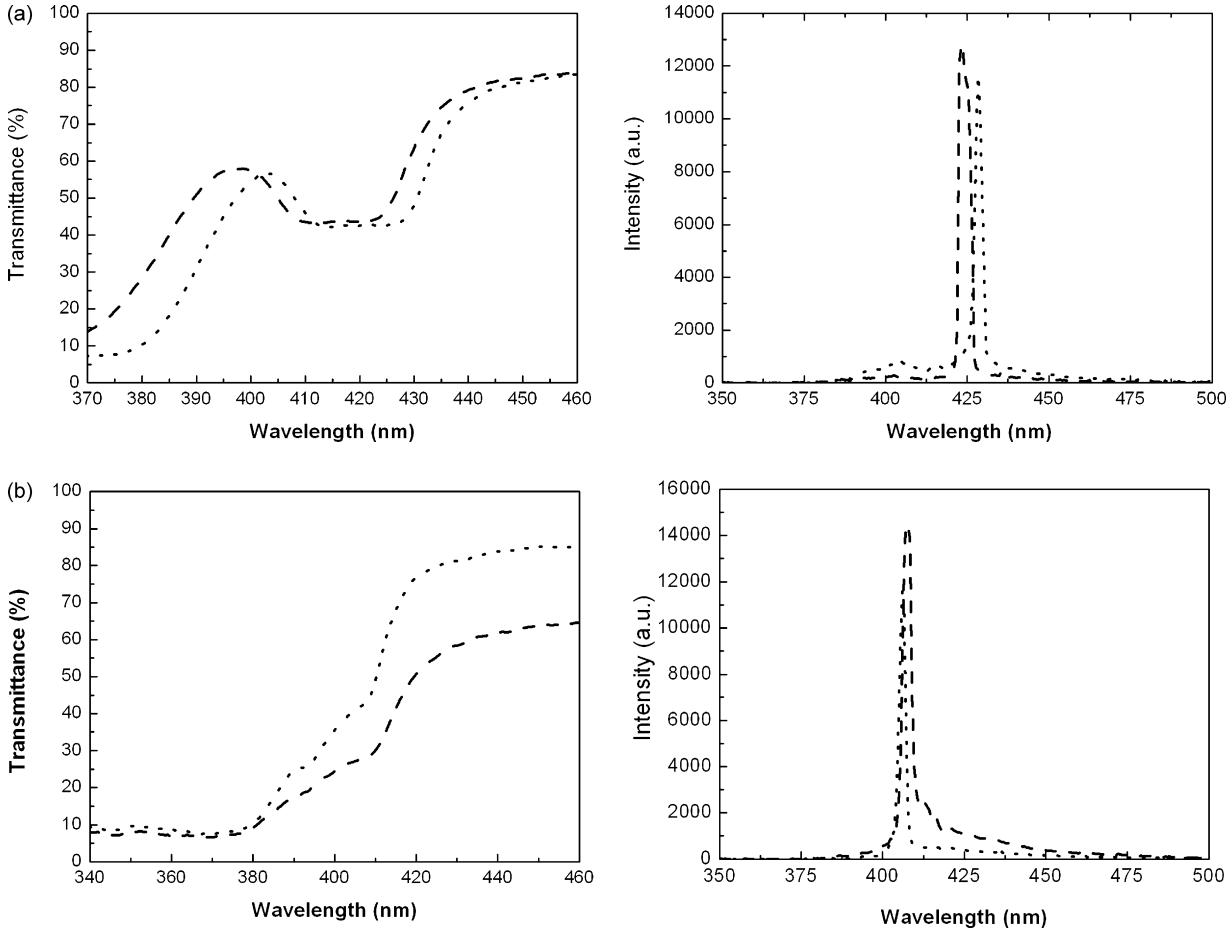

Fig. 8. (a) Photonic band gap (left) for the mixture 64% **MLC-6815** + 36% **MLC-6247** doped with 0.5% of **OF(mb)$_2$(eh)$_1$** (dashed line) and with 1.3% of the same compound (dotted line) and the laser peaks (right) emitted from the doped mixtures. (b) Photonic band gap (left) for the mixture 62.5% **MLC-6816** + 37.5% **MLC-6248** doped with 0.5% of **OF(mb)$_2$(eh)$_1$** (dashed line) and with 1% of the same compound (dotted line) and the laser peaks (right) emitted from the doped mixtures.

laser peaks emitted from the doped mixtures. In Fig. 7b it is shown the photonic band gap shift obtained doping the mixture 64.5% **MLC-6816** + 35.5% **MLC-6248** (solid line) with 0.5% of **OF(mb)$_2$(o)$_1$** (dashed line) and with 1% of the same compound (dotted line) and the laser peaks emitted from the doped mixtures.

For **OF(mb)$_2$(o)$_1$** a very tiny shift of the photonic band gap is observed for the right hand chiral mixture, we can conclude that the helical twisting power of this compound is small. This aspect is reflected in the laser emission spectra, the emitted wavelength does not shift varying the concentration of the chiral luminescent material and the emission spectra are superimposed one to the other. The difficulties in the evaluation of the laser wavelength may also be attributed to the low resolution of the used spectrometer. The observed broadening and deformation of the photonic band gap is due to the absorption of the chromophore.

Fig. 8a shows the photonic band gap shift obtained doping the mixture 64% **MLC-6815** + 36% **MLC-6247** with 0.5% of **OF(mb)$_2$(eh)$_1$** (dashed line) and with 1.3% of the same compound (dotted line) and the laser peaks emitted from the doped mixtures. Fig. 8b shows the photonic band gap shift obtained doping the mixture 62.5% **MLC-6816** + 37.5% **MLC-6248** with 0.5% of **OF(mb)$_2$(eh)$_1$** (dashed line) and with 1% of the same compound (dotted line) and the laser peaks emitted from the doped mixtures.

For **OF(mb)$_2$(eh)$_1$** it is difficult to appreciate the shift of the photonic band gap when the chiral dye is added to the right hand cholesteric mixture. Instead, adding 1% of material there is a 5 nm shift of the reflected wavelengths for the left hand starting cholesteric mixture. Since the photonic band gap for the right hand cholesteric mixture shifts towards smaller wavelengths when adding a small amount of the chiral dye, **OF(mb)$_2$(eh)$_1$** reveals to have a right hand chirality. Accordingly to the previous considerations, the tuning of the laser emission is more evident for the right hand cholesteric mixture than for the left hand one. The laser linewidth is about 5 nm as the observed shift of the laser peak.

Fig. 9a shows the photonic band gap shift obtained doping the mixture 62% **MLC-6816** + 38% **MLC-6247** with 0.5% of **OF(mb)$_n$** (dashed line) and with 1% of the same compound (dotted line) and the laser peaks emitted from the doped mixtures; in Fig. 9b it is shown the photonic band gap shift obtained doping the mixture 64.5% **MLC-6816** + 35.5% **MLC-6248** with 0.5% of **OF(mb)$_n$** (dashed line) and with 1% of the same compound (dotted line) and the laser peaks emitted from the doped mixtures.

From the transmission spectra of the mixtures we can conclude that the chiral dye **OF(mb)$_n$** is right handed, in fact, for the left handed cholesteric mixture containing **MLC-6247** we observe a shift towards longer wavelengths while for the mixture containing **MLC-6248** we observe a shift towards smaller wavelengths. As in the previous cases, the shift towards longer wavelengths is much more evident and more pronounced with respect to the one observed for the previous chiral luminescent materials. This is due to the fact that it is energetically easier to unwind a helix more than to wind it. For the left handed cholesteric mixture the range of laser tuning is around 7 nm, while for the right handed mixture is 5 nm. We can also notice that the laser emission is more intense when the cholesteric mixture is doped with the 0.5% of the chiral luminescent material. This may be due to the intrinsic fluctuations of the laser based on dye doped cholesteric liquid crystals but may be also due to the aggregation of the dye molecules or to self-quenching.

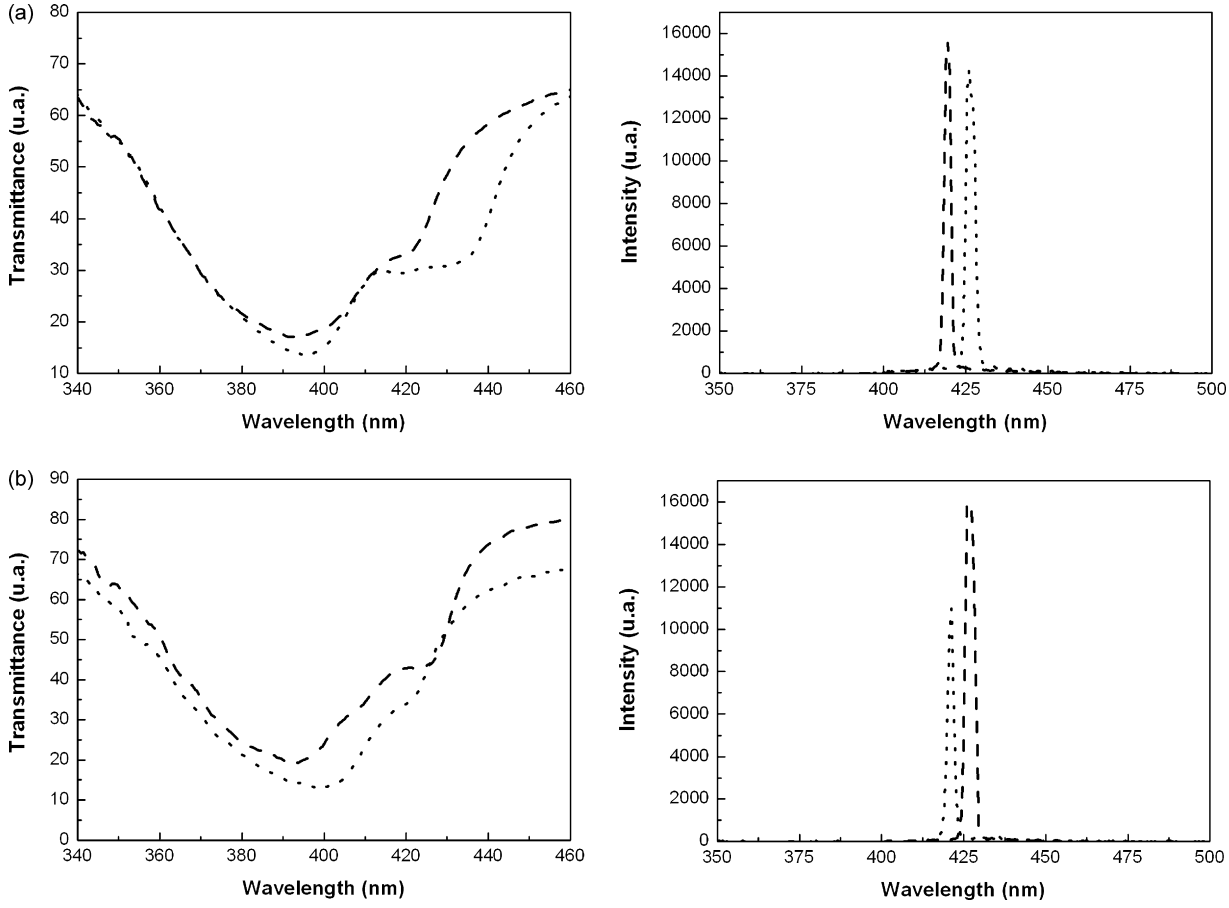

Fig. 9. (a) Photonic band gap (left) for the mixture 62% **MLC-6816** + 38% **MLC-6247** doped with 0.5% of **OF(mb)$_n$** (dashed line) and with 1% of the same compound (dotted line) and the laser peaks (right) emitted from the doped mixtures. (b) Photonic band gap (left) for the mixture 64.5% **MLC-6816** + 35.5% **MLC-6248** doped with 0.5% of **OF(mb)$_n$** (dashed line) and with 1% of the same compound (dotted line) and the laser peaks (right) emitted from the doped mixtures.

4. Conclusions

We have undertaken the synthesis and characterization of a series of monodispersed oligofluorenes and polydispersed oligo- and polyfluorenes where the aromatic core length and the structure of the appended alkyl chains at the C9 position of the fluorene core have been modified. The compounds are very efficient emitters both in solution and film with emission efficiencies, in solution, of ≈0.8 when the aromatic core consists of three or more fluorene units. The investigated oligofluorenes up to the pentamer resist crystallization and are compatible with liquid crystalline matrixes at least up to 5%. The related polyfluorene and polydispersed oligofluorene, **PF(o)$_n$** and **OF(mb)$_n$** respectively, are liquid crystals. Variations in the structure of the pendant alky chains can be used as the strategy to modulate thermal behaviour and chirality.

We have used these materials as chiral luminescent compound in DD CLCs mixtures, and the twisting power of **OF(mb)$_n$** has been proved. The same applies for **OF(mb)$_2$(eh)$_1$** where the chiral chains are combined with the racemic 2-ethylhexyl ones but the helical twisting power is reduced when the chiral chains are combined with the linear *n*-octyl ones in **OF(mb)$_2$(o)$_1$**. We have demonstrated laser emission and wavelength tuning from the cholesteric mixtures.

This kind of materials can be further optimized in order to have a stronger helical twisting power, to contain photosensitive moieties, and to have emission in different ranges of the optical spectrum by changing the chromophore.

Acknowledgments

The UZ acknowledges financial support from MEC-FEDER Spanish projects under the project MAT2008-06522-C02-01 and HI2005-0258 (Spain-Italy cooperation program), from the *Departamento de Ciencia, Tecnología y Universidad* of the Government of Aragón and FEDER founding. J. del Barrio acknowledges his grant from Government of Aragón.

The UC authors acknowledge Dr. Alfredo Pane for his technical support. This work was partially supported from the MIUR (Azioni Integrate Italia–Spagna, 2005) project: "Wide range tunable UV–vis cholesteric liquid crystal micro-laser".

References

[1] A.C. Grimsdale, K.L. Chan, R.E. Martin, P.G. Jokisz, A.B. Holmes, Chem. Rev. 109 (2009) 897.
[2] A.C. Grimsdale, K. Müllen, Macromol. Rapid. Commun. 28 (2007) 1676.
[3] U. Scherf, E.J.W. List, Adv. Mater. 14 (2002) 477.
[4] D. Neher, Macromol. Rapid. Commun. 22 (2001) 1366.
[5] M. Millaruelo, L.S. Chinellato, J.L. Serrano, L. Oriol, M. Piñol, J. Polym. Sci.: Part A. Polym. Chem. 45 (2007) 4804.
[6] M. Millaruelo, L. Oriol, J.L. Serrano, M. Piñol, P.L. Sáez, Mol. Cryst. Liq. Cryst. 411 (2004) 451.
[7] M. Millaruelo, L. Oriol, M. Piñol, P.L. Sáez, J.L. Serrano, J. Photochem. Photobiol. A: Chem. 155 (2003) 29.
[8] G. Petriashvili, G. Chilaya, M.A. Matranga, M.P. De Santo, G. Cozza, R. Barberi, J. del Barrio, L.S. Chinelatto Jr., L. Oriol, M. Piñol, Opt. Mater. 31 (2009) 1693.
[9] V.I. Kopp, Z.-Q. Zhang, A.Z. Genack, Prog. Quantum Electron 27 (2003) 369.
[10] L.S. Goldberg, J.M. Schnur US Patent 3 771 065, 1973.
[11] I.P. Il'chishin, E.A. Tikhonov, V.G. Tishchenko, M.T. Shpak, Sov. JETP Lett. 32 (1980) 24.
[12] H. Finkelmann, S.T. Kim, A. Munoz, P. Palffy-Muhoray, B. Taheri, Adv. Mater. 13 (2001) 1069.
[13] S. Furumi, S. Yokoyama, A. Otomo, S. Mashiko, Appl. Phys. Lett. 82 (2003) 16.
[14] A. Chanishvili, G. Chilaya, G. Petriashvili, R. Barberi, R. Bartolino, G. Cipparrone, A. Mazzulla, L. Oriol, Appl. Phys. Lett. 83 (2003) 5353.
[15] G. Chilaya, A. Chanishvili, G. Petriashvili, R. Barberi, R. Bartolino, M.P. De Santo, M.A. Matranga, P. Collings, Mol. Cryst. Liq. Cryst. 453 (2006) 123.
[16] A. Chanishvili, G. Chilaya, G. Petriashvili, R. Barberi, R. Bartolino, G. Cipparrone, A. Mazzulla, L. Oriol, Adv. Mater. 16 (2004) 791.
[17] A. Chanishvili, G. Chilaya, G. Petriashvili, R. Barberi, R. Bartolino, G. Cipparrone, A. Mazzulla, R. Gimenez, L. Oriol, M. Pinol, Appl. Phys. Lett. 86 (2005), 051107 (1–3).
[18] M. Grell, D.D.C. Bradley, M. Insbasekaran, E.P. Woo, Adv. Mater. 9 (1997) 798.
[19] Y. Geng, S.W. Culligan, A. Trajkovska, J.U. Wallace, S.H. Chen, Chem. Mater. 15 (2003) 542.
[20] Y. Geng, A. Trajkovska, S.W. Culligan, J.J. Ou, H.M.P. Chen, D. Katsis, S.H. Chen, J. Am. Chem. Soc. 125 (2003) 14032.
[21] Y. Geng, A. Trajkovska, D. Katsis, J.J. Ou, S.W. Culligan, S.H. Chen, J. Am. Chem. Soc. 124 (2002) 8337.
[22] F. Araoka, K.-C. Shin, Y. Takanishi, K. Ishikawa, H. Takezoe, Z. Zhu, T.M. Swager, J. Appl. Phys. 94 (2003) 279.
[23] K.-C. Shin, F. Araoka, B. Park, Y. Takanishi, K. Ishikawa, Z. Zhu, T.M. Swager, H. Takezoe, Jpn. J. Appl. Phys. 43 (2004) 631.
[24] D. Katsis, Y.H. Geng, J.J. Ou, S.W. Culligan, A. Trajkovska, S.H. Chen, L.J. Rothberg, Chem. Mater. 14 (2002) 1332.
[25] R. Gimenez, L. Oriol, M. Pinol, J.L. Serrano, A.I. Vinuales, T. Fisher, J. Stumpe, Helv. Chim. Acta 89 (2006) 304.
[26] D. Eaton, Pure Appl. Chem. 60 (1988) 1107.
[27] A. Suzuki, Pure Appl. Chem. 63 (1991) 419.
[28] J. Jo, C. Chi, S. Höger, G. Wegner, D.Y. Yoon, Chem. Eur. J. 10 (2004) 2681.
[29] G. Klarner, R.D. Miller, Macromolecules 31 (1998) 2007.
[30] J. Teetsov, M.A. Fox, J. Mater. Chem. 9 (1999) 2117.